

THE PHYSICS OF TIBETAN SINGING BOWLS

PART 1: THEORETICAL MODEL

PACS: 43.75.Kk

Inácio, Octávio¹; Henrique, Luís¹; Antunes, José²

¹ Escola Superior de Música e Artes do Espectáculo, Instituto Politécnico do Porto
Laboratório de Acústica Musical, Rua da Alegria, 503, 4000-045 Porto, Portugal
Tel: (351) 225193760, Fax: (351) 225180774
Email: Octaviolnacio@esmae-ipp.pt; LuisLeite@esmae-ipp.pt

² Instituto Tecnológico e Nuclear
Applied Dynamics Laboratory
ITN/ADL, Estrada Nacional 10, 2686-953 Sacavém Codex, Portugal
Tel: (351) 219946142, Fax: (351) 219941039, Email: jantunes@itn.mces.pt

ABSTRACT

Tibetan bowls have been traditionally used for ceremonial and meditation purposes, but are also increasingly being used in contemporary music-making. They are handcrafted using alloys of several metals and produce different tones, depending on the alloy composition, their shape, size and weight. Most important is the sound producing technique used – either impacting or rubbing, or both simultaneously – as well as the excitation location, the hardness and friction characteristics of the exciting stick (called *puja*).

Quite recently, researchers became interested in the physical modelling of singing bowls, using waveguide synthesis techniques for performing numerical simulations. Their efforts aimed particularly at achieving real-time synthesis and, as a consequence, several aspects of the physics of these instruments do not appear to be clarified in the published formulations and results.

In this paper, we extend to axi-symmetrical shells – subjected to impact and friction-induced excitations – our modal techniques of physical modelling, which were already used in previous papers concerning plucked and bowed strings as well as impacted and bowed bars. We start by an experimental modal identification of three different Tibetan bowls, and then develop a modelling approach for Tibetan bowls. Extensive nonlinear numerical simulations were performed, for both impacted and rubbed bowls, which are presented in a companion paper.

INTRODUCTION

Singing bowls are traditionally made in Tibet, Nepal, India, China and Japan. Although the name *qing* has been applied to lithophones since the Han Chinese Confucian rituals, more recently it also designates the bowls used in Buddhist temples. In the Himalaya there is a very ancient tradition of metal manufacture, and bowls have been handcrafted using alloys of several metals – mainly copper and tin, but also other metals such as gold, silver, iron, lead, etc. – each one believed to possess particular spiritual powers. There are many distinct bowls, which produce different tones, depending on the alloy composition, their shape, size and weight. Most important is the sound producing technique used – either impacting or rubbing, or both simultaneously – as well as the excitation location, the hardness and friction characteristics of the exciting stick (called *puja*, frequently made of wood and eventually covered with a soft skin). Tibetan bowls have been used essentially for ceremonial and meditation purposes. Nevertheless, these amazing instruments are increasingly being used in contemporary music.

Quite recently, some researchers became interested in the physical modelling of singing bowls, using waveguide synthesis techniques for performing numerical simulations [1-3]. Their efforts aimed particularly at achieving real-time synthesis. Therefore, understandably, several aspects of the physics of these instruments do not appear to be clarified in the published formulations and results. For instance, to our best knowledge, an account of the radial and tangential vibratory motion components of the bowl shell – and their dynamical coupling – has been ignored in the published literature. Also, how these motion components relate to the travelling position of the *puja* contact point is not clear at the present time. Details of the contact/friction interaction models used in simulations have been seldom provided, and the significance of the various model parameters has not been asserted. On the other hand, experiments clearly show that beating phenomena arises even for near-perfectly symmetrical bowls, an important aspect which the published modelling techniques seem to miss (although beating from closely mistuned modes has been addressed – not without some difficulty [3] – but this is a quite different aspect). Therefore, it appears that several important aspects of the excitation mechanism in singing bowls still lack clarification.

In this paper, we extend to axi-symmetrical shells – subjected to impact and friction-induced excitations – our modal techniques of physical modelling, which were already used in previous papers concerning plucked and bowed strings [4-7] as well as impacted and bowed bars [7-10]. Our approach is based on a modal representation of the unconstrained system – here consisting on two orthogonal families of modes of similar (or near-similar) frequencies and shapes. The bowl modeshapes have radial and tangential motion components, which are prone to be excited by the normal and frictional contact forces between the bowl and the impact/sliding *puja*. At each time step, the generalized (modal) excitations are computed by projecting the normal and tangential interaction forces on the modal basis. Then, time-step integration of the modal differential equations is performed using an explicit algorithm. The physical motions at the contact location (and any other selected points) are obtained by modal superposition. This enables the computation of the motion-dependent interaction forces, and the integration proceeds. Details on the specificities of the contact and frictional models used in our simulations are given. An experimental modal identification has been performed for three different Tibetan bowls (Figure 1), the main results of which are supplied. Then, we produce an extensive series of nonlinear numerical simulations, for both impacted and rubbed bowls, showing the influence of the contact/friction parameters on the dynamical responses. From our computations, sounds and animations have been produced, which are reported in a companion paper [11].



Figure 1 – Picture of the three singing bowls and *pujas* used in the experiments:
Bowl 1 ($\phi = 180$ mm) ; Bowl 2 ($\phi = 152$ mm); Bowl 3 ($\phi = 140$ mm).

EXPERIMENTAL MODAL IDENTIFICATION

In order to estimate the natural frequencies ω_n , damping values ζ_n , modal masses m_n and modeshapes $\varphi_n(\theta, z)$ to be used in the numerical simulations, an experimental modal identification based on impact testing was performed for three bowls. A mesh of 120 test locations was defined for each instrument (e.g., 24 points regularly spaced azimuthally, at 5 different heights). Impact excitation was performed on all of the points and the radial responses

were measured by two accelerometers attached to inner side of the bowl at two positions, located at the same horizontal plane (near the rim) with a relative angle of 55° between them, as can be seen in Figure 2(a). Modal identification was achieved by developing a MDOF algorithm in the frequency domain [12]. The modal parameters were optimized in order to minimize the error $\varepsilon(\omega_n, \zeta_n, m_n, \varphi_n)$ between the measured transfer functions $H_{er}(\omega) = \dot{Y}_r(\omega)/F_e(\omega)$ and the fitted modal model $\hat{H}_{er}(\omega; \omega_n, \zeta_n, m_n, \varphi_n)$, for all measurements (P_e excitation and P_r response locations), in a given frequency range $[\omega_{\min}, \omega_{\max}]$ encompassing N modes. Hence:

$$\varepsilon(\omega_n, \zeta_n, m_n, \varphi_n) = \sum_{e=1}^{P_e} \sum_{r=1}^{P_r} \int_{\omega_{\min}}^{\omega_{\max}} \left[H_{er}(\omega) - \hat{H}_{er}(\omega; \omega_n, \zeta_n, m_n, \varphi_n) \right] d\omega \quad (1)$$

with:

$$\hat{H}_{er}(\omega; \omega_n, \zeta_n, m_n, \varphi_n) = \sum_{n=n_1}^{n_1+N} -\omega^2 \frac{A_n^{er}}{\omega_n^2 - \omega^2 + 2i\omega\omega_n\zeta_n} - \omega^2 C_1 + C_2 \quad (2)$$

where the modal amplitude coefficients are given as $A_n^{er} = \varphi_n(\theta_e, z_e)\varphi_n(\theta_r, z_r)/m_n$ and the two last terms in (2) account for modes located out of the identified frequency-range. The values of the modal masses obviously depend on how modeshapes are normalized (we used $|\varphi(\theta, z)|_{\max} = 1$). Note that the identification is nonlinear in ω_n and ζ_n but linear in A_n^{er} .

Results from the experiments on the three bowls show the existence of 5 to 7 prominent resonances with very low modal damping values up to frequencies about 4 ~ 6 kHz. As an illustration, Figure 2(b) depicts the modulus of a frequency response function obtained from Bowl 2, relating the acceleration measured at point 1 to the force applied at the same point.

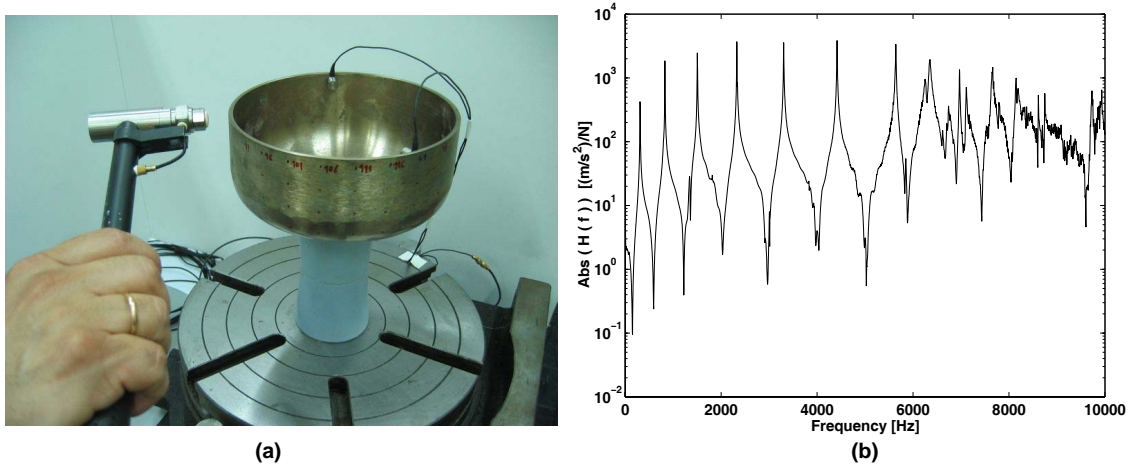


Figure 2 – Experimental modal identification of bowl 2: (a) Picture showing the measurement grid and accelerometer locations; (b) Modulus of the acceleration frequency response function

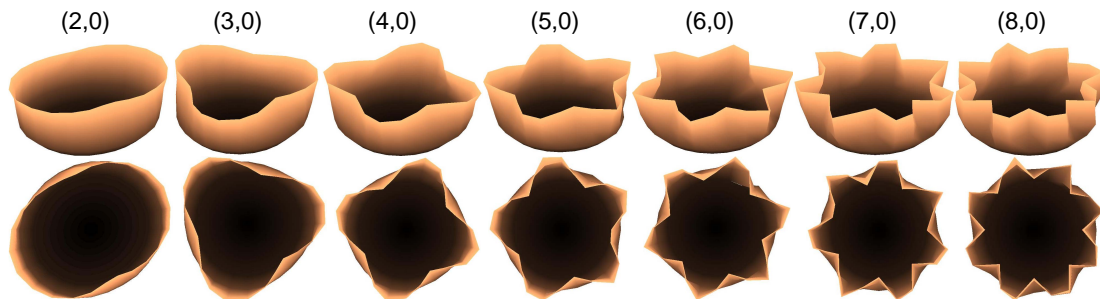


Figure 3 – Experimentally identified modeshapes (j,k) of the first 7 elastic modes of Bowl 2 (j relates to the number of nodal meridians and k to the number nodal circles – see text)

The shapes of the identified bowl modes are mainly due to bending waves that propagate azimuthally, resulting in patterns similar to some modeshapes of bells [13]. Following Rossing, notation (j,k) represents here the number of complete nodal meridians extending over the top of the bowl (half the number of nodes observed along a circumference), and the number of nodal

circles, respectively. Figure 3 shows perspective and top views of the first 7 “sounding” modeshapes (rigid-body modes are not shown) for Bowl 2, as extracted from experiments. In the frequency-range explored, all the identified modes are of the $(j,0)$ type, due to the low value of the height to diameter ratio (Z/ϕ) for Tibetan bowls, in contrast to most bells.

Although modal frequencies and damping values were obtained from the modal identification routine, it was soon realized that the accelerometers and their cables had a non-negligible influence on the bowl modal parameters (the very low damping was particularly affected by the instrumentation). Indeed, measurements of the near-field sound pressure radiated by impacted bowls showed slightly higher values for the natural frequencies and much longer decay times, when compared to those displayed after transducers were installed. Hence, we decided to use the modal parameters identified from the acoustic responses of non-instrumented impacted bowls. Modal frequencies were extracted from the sound pressure spectra and damping values were computed from the logarithm-decrement of band-pass filtered (at each mode) sound pressure decays.

Table 1 shows the values of the modal frequencies for the most prominent modes of the three bowls tested, together with their ratios to the fundamental – mode $(2,0)$ –, which are entirely in agreement with the results obtained by Rossing [13]. Interestingly, these ratios are rather similar, in spite of the different bowl shapes, sizes and wall depths. The frequency relationships are mildly inharmonic, which does not affect the definite pitch of this instrument, mainly dominated by the first $(2,0)$ shell mode. As stated, dissipation is very low, with modal damping ratios typically in the range $\zeta_n = 0.002 \sim 0.015 \%$ (higher values pertaining to higher-order modes). However, note that these values may increase one order of magnitude, or more, depending on how the bowls are actually supported or handled.

Table 1 – Modal frequencies and frequency ratios of the three bowls

Mode	Bowl 1 ($m_T = 934 \text{ g}$, $\phi = 180 \text{ mm}$)		Bowl 2 ($m_T = 563 \text{ g}$, $\phi = 152 \text{ mm}$)		Bowl 3 ($m_T = 557 \text{ g}$, $\phi = 140 \text{ mm}$)	
	f_n [Hz]	f_n/f_1	f_n [Hz]	f_n/f_1	f_n [Hz]	f_n/f_1
(2,0)	221	1,0	314	1,0	528	1,0
(3,0)	614	2,8	836	2,7	1460	2,8
(4,0)	1145	5,2	1519	4,8	2704	5,1
(5,0)	1804	8,1	2360	7,5	4122	7,8
(6,0)	2577	11,6	3341	10,7	5694	10,8
(7,0)	3456	15,6	4462	14,2	-	-
(8,0)	4419	20,0	5696	18,2	-	-

FORMULATION OF THE DYNAMICAL SYSTEM

Dynamical Formulation of the Bowl in Modal Coordinates

Perfectly axi-symmetrical structures exhibit double vibrational modes, occurring in orthogonal pairs with identical frequencies ($\omega_n^A = \omega_n^B$) [14]. However, if a slight alteration of this symmetry is introduced, the natural frequencies of these two degenerate modal families deviate from identical values by a certain amount $\Delta\omega_n$. The use of these modal pairs is essential for the correct dynamical description of axi-symmetric bodies, under general excitation conditions. Furthermore, shell modeshapes present both radial and tangential components. Figure 4 displays a representation of the first four modeshape pairs, near the bowl rim, where the excitations are usually exerted (e.g., $z_e \approx Z$). Both the radial (green) and tangential (red) motion components are plotted, which for geometrically perfect bowls can be formulated as:

$$\varphi_n^A(\theta) = \varphi_n^{Ar}(\theta) \vec{r} + \varphi_n^{At}(\theta) \vec{t} \quad \text{and} \quad \varphi_n^B(\theta) = \varphi_n^{Br}(\theta) \vec{r} + \varphi_n^{Bt}(\theta) \vec{t} \quad (3,4)$$

$$\text{with} \quad \begin{cases} \varphi_n^{Ar}(\theta) = \cos(n\theta) \\ \varphi_n^{At}(\theta) = -\sin(n\theta)/n \end{cases} ; \quad \begin{cases} \varphi_n^{Br}(\theta) = \sin(n\theta) \\ \varphi_n^{Bt}(\theta) = \cos(n\theta)/n \end{cases} \quad (5,6)$$

where $\varphi_n^{Ar}(\theta)$ corresponds to the radial component of the A family n th modeshape, $\varphi_n^{At}(\theta)$ to the tangential component of the A family n th mode shape, etc. Figure 4 shows that spatial phase angles between orthogonal mode pairs are $\pi/2j$. One immediate conclusion can be drawn from the polar diagrams shown and equations (5,6): the amplitude of the tangential modal component decreases relatively to the amplitude of the radial component as the mode number increases. This suggests that only the lower-order modes are prone to engage in self-sustained motion due to tangential rubbing excitation by the *puja*.

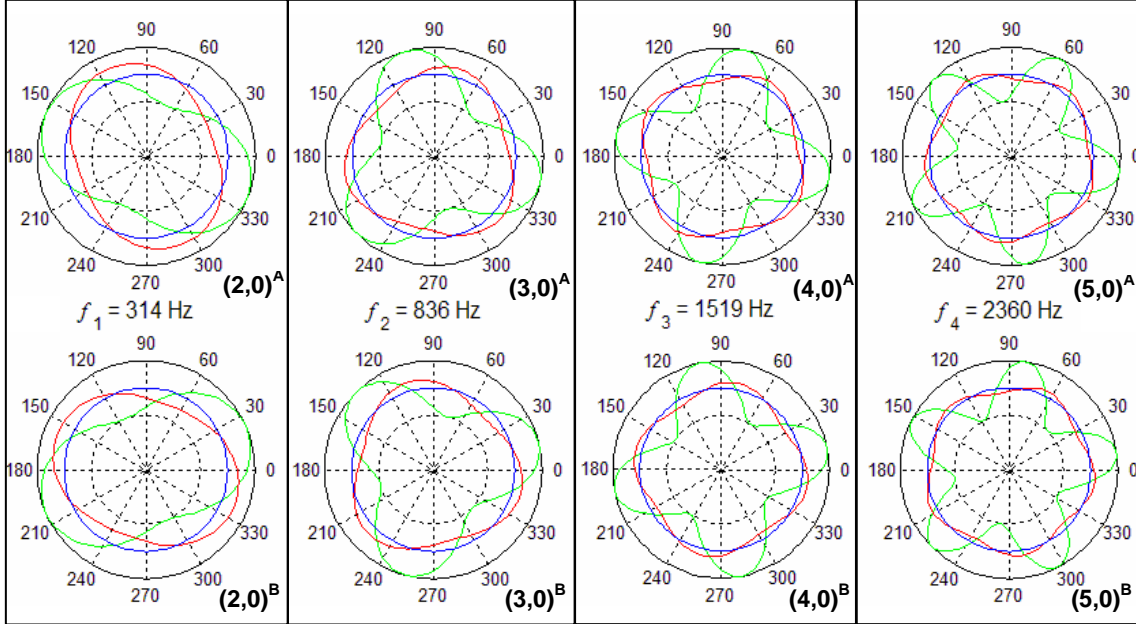


Figure 4 – Mode shapes at the bowl rim of the first four orthogonal mode pairs (Blue: Undeformed; Green: Radial component; Red: Tangential component)

If linear dissipation is assumed, the motion of the system can be described in terms of the bowl's two families of modal parameters: modal masses m_n^X , modal circular frequencies ω_n^X , modal damping ζ_n^X , and mode shapes $\varphi_n^X(\theta)$ (at the assumed excitation level $z_e \approx Z$), with $n = 1, 2, \dots, N$, where X stands for the modal family A or B . The order N of the modal truncation is problem-dependent and should be asserted by physical reasoning, supported by the convergence of computational results. The maximum modal frequency to be included, ω_N , mostly depends on the short time-scales induced by the contact parameters – all modes significantly excited by impact and/or friction phenomena should be included in the computational modal basis.

The forced response of the damped bowl can then be formulated as a set of $2N$ ordinary second-order differential equations:

$$\begin{bmatrix} [M_A] & 0 \\ 0 & [M_B] \end{bmatrix} \begin{Bmatrix} \{\ddot{Q}_A(t)\} \\ \{\ddot{Q}_B(t)\} \end{Bmatrix} + \begin{bmatrix} [C_A] & 0 \\ 0 & [C_B] \end{bmatrix} \begin{Bmatrix} \{\dot{Q}_A(t)\} \\ \{\dot{Q}_B(t)\} \end{Bmatrix} + \begin{bmatrix} [K_A] & 0 \\ 0 & [K_B] \end{bmatrix} \begin{Bmatrix} \{Q_A(t)\} \\ \{Q_B(t)\} \end{Bmatrix} = \begin{Bmatrix} \{\Xi_A(t)\} \\ \{\Xi_B(t)\} \end{Bmatrix} \quad (7)$$

where:

$[M_X] = \text{Diag}(m_1^X, \dots, m_N^X)$, $[C_X] = \text{Diag}(2m_1^X \omega_1^X \zeta_1^X, \dots, 2m_N^X \omega_N^X \zeta_N^X)$, $[K_X] = \text{Diag}(m_1^X (\omega_1^X)^2, \dots, m_N^X (\omega_N^X)^2)$ are the matrices of the modal parameters (where X stands for A or B), for each of the two orthogonal mode families, while $\{Q_X(t)\} = \langle q_1^X(t), \dots, q_N^X(t) \rangle^T$ and $\{\Xi_X(t)\} = \langle \mathfrak{S}_1^X(t), \dots, \mathfrak{S}_N^X(t) \rangle^T$ are the vectors of the modal responses and of the generalized forces, respectively. Note that, although equations (7) obviously pertain to a linear formulation, nothing prevents us from including in $\mathfrak{S}_n^X(t)$ all the nonlinear effects which arise from the contact/friction interaction between the bowl and the *puja*. Accordingly, the system modes become coupled by such nonlinear effects.

The modal forces $\mathfrak{F}_n^x(t)$ are obtained by projecting the external force field on the modal basis:

$$\mathfrak{F}_n^x(t) = \int_0^{2\pi} \left[F_r(\theta, t) \varphi_n^{Xr}(\theta) + F_t(\theta, t) \varphi_n^{Xt}(\theta) \right] d\theta \quad ; \quad n=1, 2, \dots, N \quad (8)$$

where $F_r(\theta, t)$ and $F_t(\theta, t)$ are the radial (impact) and tangential (friction) force fields applied by the *puja* – e.g., a localised impact $F_r(\theta_c, t)$ and/or a travelling rub $F_{r,t}(\theta_c(t), t)$. The radial and tangential physical motions can be then computed at any location θ from the modal amplitudes $q_n^x(t)$ by superposition:

$$y_r(t) = \sum_{n=1}^N \left[\varphi_n^{Ar}(\theta) \cdot q_n^A(t) + \varphi_n^{Br}(\theta) \cdot q_n^B(t) \right] \quad ; \quad y_t(t) = \sum_{n=1}^N \left[\varphi_n^{At}(\theta) \cdot q_n^A(t) + \varphi_n^{Bt}(\theta) \cdot q_n^B(t) \right] \quad (9,10)$$

and similarly concerning the velocities and accelerations.

Dynamics of the *Puja* and Force Field Formulation

As mentioned before, the excitation of these musical instruments can be performed in two basic different ways: by impact or by rubbing around the rim of the bowl with the *puja* (these two types of excitation can obviously be mixed, resulting in musically interesting effects). The dynamics of the *puja* will be formulated simply in terms of a mass m_p subjected to a normal (e.g. radial) force $F_N(t)$ and an *imposed* tangential rubbing velocity $V_T(t)$ – which will be assumed constant in time for all our exploratory simulations [11] – as well as to an initial impact velocity in the radial direction $V_N(t_0)$. These three parameters will be assumed controlled by the musician, and many distinct sounds may be obtained by changing them: in particular, $V_N(t_0) \neq 0$ with $F_N = V_T = 0$ will be “pure” impact, and $F_N(t) \neq 0, V_T(t) \neq 0$ with $V_N(t_0) = 0$ will be “pure” *singing* (see [11]). The radial motion of the *puja*, resulting from the external force applied and the impact/friction interaction with the bowl is given by:

$$m_p \ddot{y}_p = -F_N(t) + F_r(\theta, t) \quad (11)$$

Contact Interaction Formulation

The radial contact force resulting from the interaction between the *puja* and the bowl is simply modelled as a contact stiffness, eventually associated with a contact damping term:

$$F_r(\theta_c) = -K_c \tilde{y}_r(\theta_c, t) - C_c \dot{\tilde{y}}_r(\theta_c, t) \quad (12)$$

where \tilde{y}_r and $\dot{\tilde{y}}_r$ are respectively the bowl/*puja* relative radial displacement and velocity, at the (fixed or travelling) contact location $\theta_c(t)$, K_c and C_c are the contact stiffness and damping coefficients, directly related to the *puja* material. Other and more refined contact models – for instance of the hertzian type, eventually with hysteretic behaviour – could easily be implemented instead of (12). Such refinements are however not a priority here.

Friction Interaction Formulation

In previous papers we have shown the effectiveness of a friction model used for the simulation of bowed strings and bowed bars [4,9]. Such model enabled a clear distinction between sliding and adherence states, sliding friction forces being computed from the Coulomb model $F_t = -|F_r| \mu_d(\dot{\tilde{y}}_t) \text{sgn}(\dot{\tilde{y}}_t)$, where $\dot{\tilde{y}}_t$ is the the bowl/*puja* relative tangential velocity, and the adherence state being modelled essentially in terms of a local “adherence” stiffness K_a and some damping. We were thus able to emulate true friction sticking of the contacting surfaces, whenever $|F_t| < |F_r| \mu_s$, however at the expense of a longer computational time, as smaller integration time-steps seem to be imposed by the transitions from velocity-controlled sliding states to displacement-controlled adherence states.

In this paper, a simpler approach is taken to model friction interaction, which allows for faster computation times, although it lacks the capability to emulate true friction sticking. The friction force will be formulated as:

$$\begin{cases} F_t(\theta_c, t) = -|F_r(\theta_c, t)|\mu_d(\dot{\tilde{y}}_t(\theta_c, t)) \operatorname{sgn}(\dot{\tilde{y}}_t(\theta_c, t)) , & \text{if } |\dot{\tilde{y}}_t(\theta_c, t)| \geq \varepsilon \\ F_t(\theta_c, t) = -|F_r(\theta_c, t)|\mu_s \dot{\tilde{y}}_t(\theta_c, t) / \varepsilon , & \text{if } |\dot{\tilde{y}}_t(\theta_c, t)| < \varepsilon \end{cases} \quad (13)$$

where μ_s is a “static” friction coefficient and $\mu_d(\dot{\tilde{y}}_t)$ is a “dynamic” friction coefficient, which depends on the *puja*/bowl relative surface velocity $\dot{\tilde{y}}_t$. We will use the following model:

$$\mu_d(\dot{\tilde{y}}_t) = \mu_\infty + (\mu_s - \mu_\infty) \exp(-C |\dot{\tilde{y}}_t(\theta_c, t)|) \quad (14)$$

where, $0 \leq \mu_\infty \leq \mu_s$ is an asymptotic lower limit of the friction coefficient when $|\dot{\tilde{y}}_t| \rightarrow \infty$, and parameter C controls the decay rate of the friction coefficient with the relative sliding velocity, as shown in the typical plot of Figure 5(a). This model can be fitted to the available experimental friction data (obtained under the assumption of instantaneous velocity-dependence), by adjusting the empirical constants μ_s , μ_∞ and C .

Notice that both equations (13) correspond to velocity-controlled friction forces. For values of $\dot{\tilde{y}}_t$ outside the interval $[-\varepsilon, \varepsilon]$, the first equation simply states Coulomb’s model for sliding. Inside the interval $[-\varepsilon, \varepsilon]$, the second equation models a state of *pseudo-adherence* at very low tangential velocities. Obviously, ε acts as a regularization parameter for the friction force law, which replaces the “zero-velocity” discontinuity (which renders the adherence state numerically tricky), as shown in Figure 5(b). This regularization method, extensively developed in [15], has been often used as a pragmatic way to deal with friction phenomena in the context of dynamic problems. However, using this model, the friction force will always be zero at zero sliding velocity, inducing a relaxation on the “adherence” state (dependent on the magnitude of ε), and therefore disabling a true sticking behaviour. How pernicious this effect may be is problem-dependent – systems involving a prolonged adherence will obviously suffer more from the relaxation effect than systems which are sliding most of the time. These issues will be thoroughly discussed elsewhere. For the problem addressed here, we have obtained realistic results using formulation (13), for small enough values of the regularization domain (we used $\pm\varepsilon \approx 10^{-4} \text{ ms}^{-1}$) – results which do not seem to critically depend on ε (within reasonable limits).

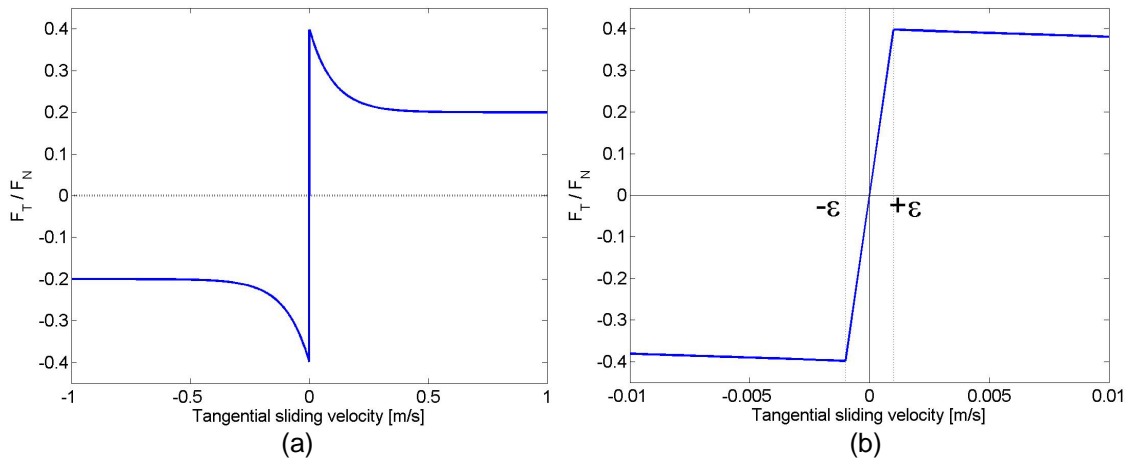


Figure 5 – Evolution of the friction coefficient with the contact relative tangential velocity ($\mu_\infty = 0.2$, $\mu_s = 0.4$, $C = 10$): (a) For $-1 < \dot{\tilde{y}}_t < 1$; (b) For $-0.01 < \dot{\tilde{y}}_t < 0.01$

Time-Step Integration

For given external excitation and initial conditions, the previous system of equations is numerically integrated using an adequate time-step algorithm. Explicit integration methods are well suited for the contact/friction model developed here. In our implementation, we used a simple Verlet integration algorithm [10], which is a low-order explicit scheme.

CONCLUSIONS

In this paper we have presented a modelling technique based on a modal approach which can achieve accurate time-domain simulations of impacted and/or rubbed axi-symmetrical structures such as the Tibetan singing bowl.

To substantiate the numerical simulations presented in a companion paper, we performed an experimental modal analysis on three bowls. Results show the existence of 5 to 7 prominent vibrational modes up to frequencies about 6 kHz, with very low modal damping values.

As a concluding note, the computational methods presented in this paper can be easily adapted for the dynamical simulation of glass harmonicas, by simply changing the modes of the computed system, as well as the contact and friction parameters.

REFERENCES

- [1] P. Cook, "Real Sound Synthesis for Interactive Applications", A. K. Peters, Natick, Massachusetts, USA (2002).
- [2] S. Serafin, C. Wilkerson, J. Smith III, "Modeling Bowl Resonators Using Circular Waveguide Networks", Proceedings of the 5th International Conference on Digital Audio Effects (DAFx-02), Hamburg, Germany (2002).
- [3] D. Young, G. Essl, "HyperPuja: A Tibetan Singing Bowl Controller", Proceedings of the Conference on New Interfaces for Musical Expression (NIME-03), Montreal, Canada (2003).
- [4] J. Antunes, M. Tafasca, L. Borsoi, "Simulation des Régimes Vibratoires Non-Linéaires d'Une Corde de Violon", Bulletin de la Société Française de Mécanique, N° 2000-3, pp. 193-202 (2000).
- [5] J. Antunes, L. Henrique, O. Inácio, "Aspects of Bowed-String Dynamics", Proceedings of the 17th International Congress on Acoustics, (ICA 2001), Roma, Italy (2001).
- [6] O. Inácio, "Largeur d'Archet et Régimes Dynamiques de la Corde Frottée", Actes du 6e Congrès Français d'Acoustique (CFA 2002), Lille, France (2002).
- [7] O. Inácio, L. Henrique, J. Antunes, "Nonlinear Dynamics and Playability of Bowed Instruments: From the Bowed String to the Bowed Bar", Proceedings of the Eleventh International Conference on Computational Methods and Experimental Measurements (CMEM 2003), Halkidiki, Greece (2003).
- [8] O. Inácio, L. Henrique, J. Antunes, "Dynamical Analysis of Bowed Bars", Proceedings of the 8th International Congress on Sound and Vibration (ICSV8), Hong Kong, China (2001).
- [9] O. Inácio, L. Henrique, J. Antunes, "Simulation of the Oscillation Regimes of Bowed Bars: A Nonlinear Modal Approach", Communications in Nonlinear Science and Numerical Simulation, Vol. 8, pp. 77-95 (2003).
- [10] L. Henrique, J. Antunes, "Optimal Design and Physical Modelling of Mallet Percussion Instruments (Parts 1 and 2)", Actes du 6e Congrès Français d'Acoustique (CFA 2002), Lille, France (2002). Also in Acta Acustica (2003, in print).
- [11] O. Inácio, L. Henrique, J. Antunes, "The Physics of Singing Bowls – Part 2: Numerical Simulations", 34º Congreso Nacional de Acústica y Encuentro Ibérico de Acústica (TecniAcustica 2003), Bilbao, España (2003).
- [12] D. J. Ewins, "Modal Testing Theory and Practice", Wiley, New York, USA (1984).
- [13] T. D. Rossing, "Science of Percussion Instruments", World Scientific, New Jersey, USA (2000).
- [14] L. A. Godoy, "Thin-Walled Structures with Structural Imperfections: Analysis and Behavior", Pergamon, Oxford, UK (1996).
- [15] J. T. Oden, J. A. C. Martins, "Models and Computational Methods for Dynamic Friction Phenomena", Comput. Methods Appl. Mech. Eng. 52, 527-634 (1985).